

INTERNATIONAL SOCIETY FOR SOIL MECHANICS AND GEOTECHNICAL ENGINEERING



This paper was downloaded from the Online Library of the International Society for Soil Mechanics and Geotechnical Engineering (ISSMGE). The library is available here:

<https://www.issmge.org/publications/online-library>

This is an open-access database that archives thousands of papers published under the Auspices of the ISSMGE and maintained by the Innovation and Development Committee of ISSMGE.

Failure mechanism and characteristics of soil subjected to interaction between soil elements in simple shear

Mécanisme des ruptures et leurs caractéristiques lors de cisaillements simples pour lesquels les éléments de terres interagissent

S. Shigemura & T. Tokue

Department of Civil Engineering, Nihon University, Japan

ABSTRACT

To clarify shear behaviour in soil elements in a shear band which undergoes interaction between soil elements, principal stress rotation, etc, a simple shear test using a large specimen with five-coupled elements was conducted with the following results: the middle three elements produce the pure shear state by interaction, and show shear behaviours similar to those in a shear band and a two-step failure mechanism in which the overall failure follows the formation of local failure surfaces; one of Coulomb's and Mohr-Coulomb's failure criteria can derive the other of the two, etc.

RÉSUMÉ

Afin d'éclaircir le comportement lors des cisaillements pour lesquels les éléments du sol interagissent au niveau de la bande de cisaillement, où il y a des contraintes principales en la rotation. Un grand échantillon test de bandes de cisaillements a été créé, composé à partir de 5 parties jointives. L'étude a donné les résultats suivants : les 3 éléments centraux provoquent un état de cisaillement pure par interaction tel qu'ils sont généralement observés au niveau de la bande de cisaillement. Le mécanisme de rupture est provoqué en deux étapes, l'une au niveau des surfaces à l'échelle locale engendrant l'autre au niveau global. Les lois de Coulomb et Mohr-Coulomb régissant ces ruptures sont déduites l'une de l'autre.

1 INTRODUCTION

The limit equilibrium method has played an important role in the solution of ground failure problems such as slope stability, bearing capacity, etc. The usual procedure in this method is to first assume a slip surface (a failure surface), and apply failure criterion for soil to the slip surface. At this time, it seems proper to use Coulomb's failure criterion considering its definition, i.e. the regular relation between stresses at failure on the "failure surface". However, the actual "slip surface" is not strictly a surface but a shear band, where the deformation of the soil is similar to that in simple shear as shown in Fig.1. It could be said, from the viewpoint of deformation, that a shear band consists of a number of soil elements in simple shear (Fig.1). As a result, neighboring soil elements in a shear band inevitably interact with each other through their boundaries. A distribution of stresses acting on the upper and lower boundary surfaces of a shear band is generally non-homogeneous owing to an unequal thickness in the overburden soil layer, rotation of principal stress axes in simple shear, etc. All the above indications suggest that the deformation and failure of soil elements in a shear band are mainly characterized by the following three factors: 1) a non-homogeneous distribution of stresses, 2) principal stress axes rotation, and 3) interaction between soil elements.

By conducting failure tests using model slopes, we have shown that in a non-homogeneous stress field failure propagation, i.e. a progressive failure, inevitably occurs even in a ductile soil slope, and that the failure propagation phenomena can be classified into *strain energy accumulated propagation* and *strain energy released propagation* by strain energy condition, and *forced propagation* and *self-excited propagation* by external force conditions (Tokue, 1999; Tokue and Shigemura, 2003). There have been studies that investigated the influence of principal stress rotation on the deformation and/or the strength of soils (e.g., Cole, 1967; Oda, 1975; Ochiai, 1975; Miura et al., 1986; Nakata et al., 1998). Most of these studies used the element test which can give only the average values of parameters over the whole of a soil specimen. Accordingly, the data

from the element test cannot exclude the influence of artificial boundaries in the specimen, and cannot include the influence of interaction between soil elements. Therefore, to obtain "true" shear behaviours such as those in a shear band, a shear test is required that reduces the influence of artificial boundaries in the specimen as much as possible, and enables interaction between soil elements. The objective of this paper is to clarify the failure mechanism and characteristics of a soil element subjected to interaction between soil elements in simple shear using a new type of simple shear apparatus.

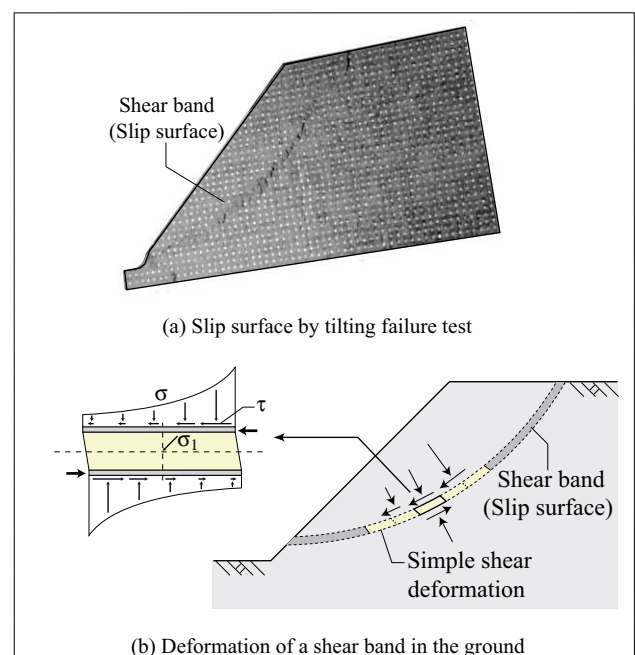


Figure 1. Slip surface and shear band

2 SIMPLE SHEAR TESTS USING A SAND SPECIMEN WITH FIVE- COUPLED ELEMENTS

We have developed a new type of simple shear apparatus using a large sand specimen $15 \times 10 \times 50$ cm consisting of five-coupled elements as shown in Fig. 2. Neighboring elements in the specimen inevitably interact with each other through their boundaries, while the middle three elements minimize the influences of artificial boundaries on the specimen. A constant overburden pressure of 49, 98 and 147 kN/m^2 was applied equally and independently to the upper loading plate of each element by a Bellofram cylinder, and shear load was applied to the specimen by sliding the bottom plate of the specimen by displacement control. The stresses on the horizontal and boundary planes of each element, (σ_{hi}, τ_{hi}) and (σ_{bi}, τ_{bi}) , as shown in Fig.3(a), can be determined by measurement and calculation because ten xy-type load cells and two x-type load cells are set on the three surfaces of the specimen (Fig.2(b)), and friction on the four surfaces of the specimen except the upper and lower surfaces is reduced to nearly zero by the friction cutting system consisting of very thin rubber and Teflon sheets, and silicone oil. Mohr's stress circle at failure of each element was determined by applying the least squares method to the stresses, (σ_{hi}, τ_{hi}) and (σ_{bi}, τ_{bi}) , and by considering the correction of shear strain γ (Fig.3(a)). Some symbols on Mohr's stress circle relating to the maximum mobilized planes are shown in Fig.3(b). A transparent acrylic plate with a thickness of 3 cm was used for the front confining wall of the specimen to allow photographs of the displacements of markers drawn at 1-centimeter spacing on the front rubber sheet of the specimen. Several kinds of strains within the sand specimen were analyzed using these photographs. The sand was Gifu sand with the following properties: specific gravity (G_s) 2.638, mean grain size (D_{50}) 0.29 mm, and maximum and minimum void ratios (e_{max} and e_{min}) 1.10 and 0.71. Dense and loose specimens were prepared with the relative densities of $D_r=95\%$ and 31% , respectively.

3 TEST RESULTS AND CONSIDERATION

In this paper we describe mainly the test results for dense specimens under a constant overburden pressure of 98 kN/m^2 owing to limited space. The test results for loose specimens showed a similar tendency to those of dense specimens.

3.1 External force condition of the specimen

Figure 4 shows that the summation of shear forces acting on the upper surfaces of the soil elements, ΣS_{topi} , is almost equal to that acting on the lower surfaces, ΣS_{bti} . Considering this, together with an adequate reduction of friction as described above, the equilibrium of horizontal forces about the specimen shows that the horizontal forces acting on the right and left side planes of the specimen cancel each other out, i.e. are numerically equal to each other. Accordingly, the external force condition of the specimen is almost ideally symmetric.

3.2 Influences of rotational moment and artificial boundaries of the specimen in simple shear

In this test, the influences of the rotational moment due to shear ought to appear in a non-homogeneous distribution of normal stresses on the lower surfaces of the elements because constant equal overburden pressures are applied to the upper surfaces of the elements. Figure 5 shows the changes of normal stresses, $\sigma_{bt1} \sim \sigma_{bt5}$, acting on the lower surfaces of the elements due to shear. It can be seen that the normal stresses on both side elements 1 and 5, σ_{bt1} and σ_{bt5} , show extreme increase and de-

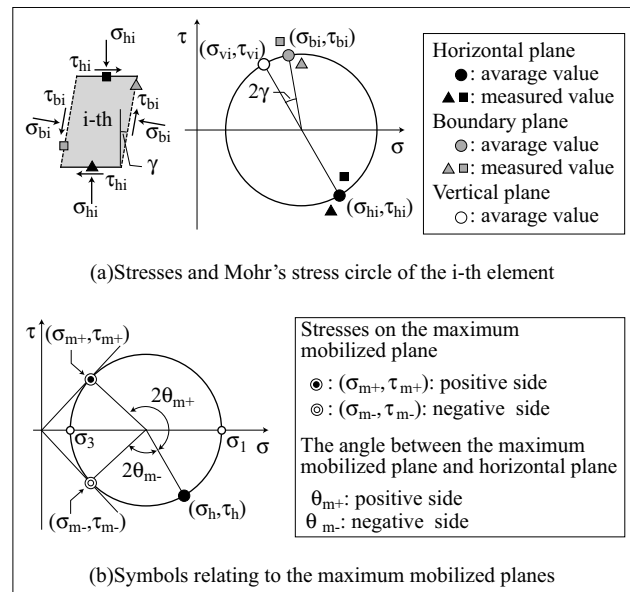
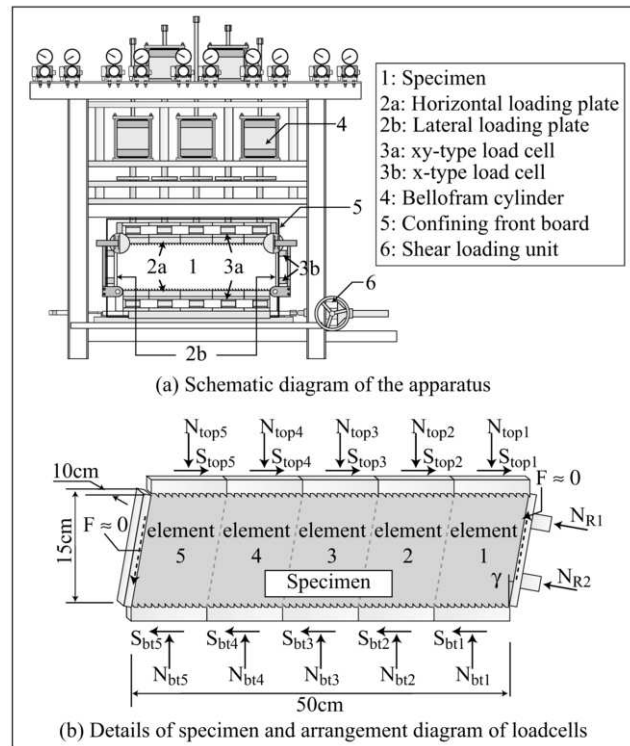


Figure 3. Determination of Mohr's stress circle and symbols relating to the maximum mobilized planes

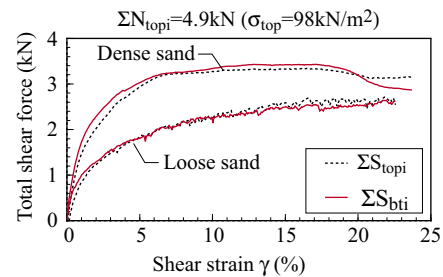


Figure 4. Total shear forces on the top and bottom planes of a specimen

decrease respectively while the normal stresses, $\sigma_{bt2} \sim \sigma_{bt4}$, of the middle three elements 2, 3 and 4 are almost equal to the constant overburden pressure. These results indicate that the influences of the rotational moment due to shear and the artificial boundaries of the specimen are found in both side elements 1 and 5, but are hardly noticed in the middle three elements 2, 3 and 4. The interaction between soil elements seems to diminish these influences in the middle three elements. Look at the detailed changes in the stresses acting on the central element 3 in Fig.6. Element 3 is in a homogeneous stress state, especially in the pure shear state from the start of shear because the normal stresses acting on each of two groups of opposite planes are almost equal, and the two sets of shear stresses acting on two groups of the opposite planes have all the same magnitude but opposite direction. As a result, we see that the middle three elements can show shear behaviours similar to those expected in a shear band. Therefore the middle three elements will henceforth be mainly examined.

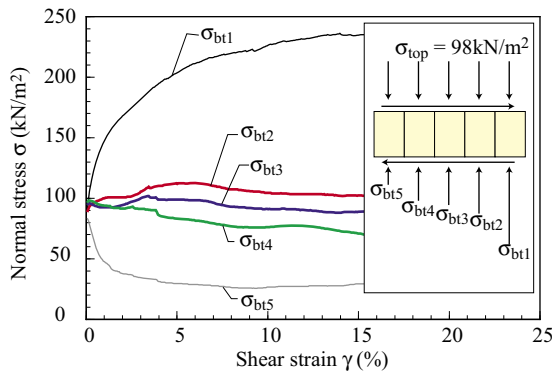


Figure 5. Normal stresses acting on the bottom planes of soil elements

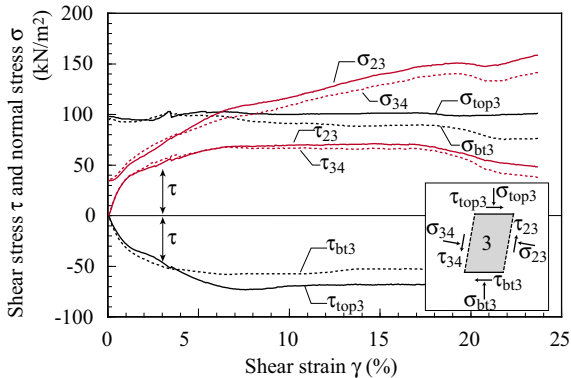


Figure 6. Changes of the stresses acting on the central element

3.3 Two-step failure mechanism

Figure 7 shows the changes of stress ratios on the horizontal plane, the boundary plane and the maximum mobilized plane of central element 3, τ_h/σ_h , τ_b/σ_b and τ_m/σ_m respectively, and the changes of angles between the maximum mobilized planes and the horizontal plane, θ_{m+} and θ_{m-} , showing the positive and negative sides as shown in Fig.3 (b).

3.3.1 Local failure at an early stage of shear

The following points can be determined from Fig. 7. At an early stage of shear with $\gamma = 1\%$: 1) the stress ratio on the boundary plane, τ_b/σ_b , peaks and agrees with the stress ratio on the maximum mobilized plane, τ_m/σ_m , and 2) as the angle θ_{m+} is almost equal to 90 degrees, the maximum mobilized plane on the positive side agrees with the vertical plane. Figure 8 shows

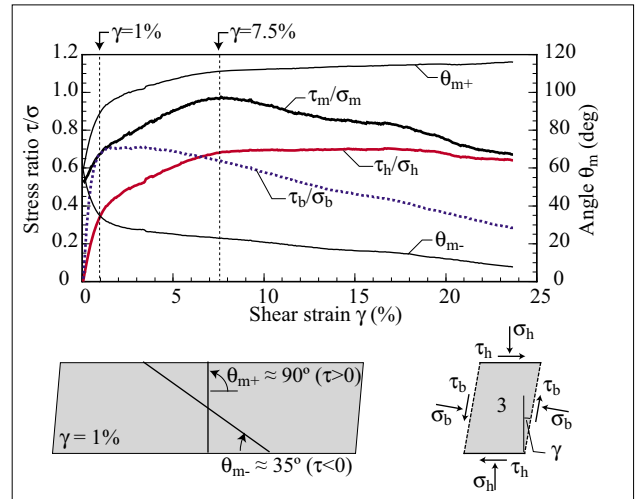


Figure 7. Changes of stress ratios and the angles between the maximum mobilized planes and horizontal plane of the central element

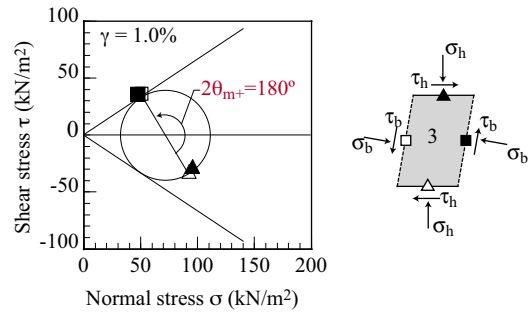


Figure 8. Mohr's stress circle at $\gamma = 1\%$ (the central element 3)

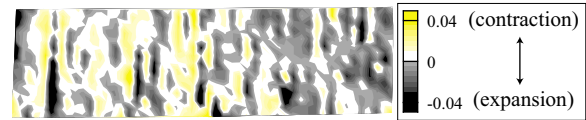


Figure 9. Distribution of normal strains on the vertical planes at $\gamma = 4.5\%$ (dense sand)

Mohr's circle of the central element 3 at $\gamma = 1\%$, which indicates that 3) the stresses on the boundary planes coincide with those on the maximum mobilized plane.

Figure 9 shows a distribution of normal strains on the vertical planes at $\gamma = 4.5\%$. It can be seen that the distribution of normal strains makes vertical stripes of expansion and contraction. Considering the results, 1) to 3) above, these vertical stripes seem to represent a number of local failure surfaces that result from the failure of the boundary surfaces on the positive side at $\gamma = 1\%$.

Figure 7 also shows that all the parameters such as the stress ratios and the angles undergo a distinct change after a turn at $\gamma = 1\%$, which suggests that the formation of these local failure surfaces significantly influences the shear behaviour of soil elements including shear strength after this formation.

3.3.2 Formation of local failure surfaces and K_0 -values

At the time of loading with overburden pressure and before shear, K_0 -values of dense and loose specimens were nearly 0.34 and 0.38 respectively. This means that the normal stress on the vertical plane (the boundary plane) is much smaller than that on the horizontal plane. On the other hand, the shear stresses on the horizontal and vertical planes were equal in magnitude and produced the pure shear state from the start of shear as indicated

in Fig.6. Therefore the stress ratio, τ/σ , increases by shear more abruptly on the vertical plane than on the horizontal plane, as is actually seen in Fig.7. This is the reason for local failure on the vertical plane at an early stage of shear for $\gamma = 1\%$. It is interesting that K_0 -values in this way remarkably affect the formation of local failure surfaces which significantly influences the shear behaviour of soil elements including shear strength.

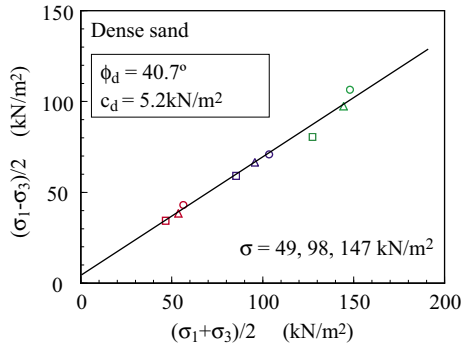


Figure 10. Mohr-Coulomb's failure criterion (dense sand)

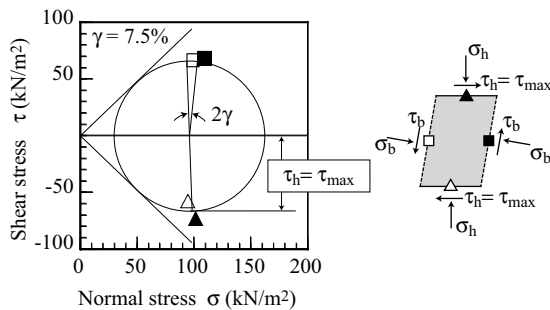


Figure 11. Mohr's stress circle at the time of overall failure of $\gamma=7.5\%$ (the central element)

3.3.3 Mechanism of overall failure

Figure 7 shows that the stress ratios on the horizontal plane and the maximum mobilized plane, τ_h/σ_h and τ_m/σ_m , peak at $\gamma = 7.5\%$. Figure 10 shows that Mohr-Coulomb's failure criterion line almost passes through the origin because the cohesion, c_d , is very small. As a result, a tangential line to Mohr's circle at the peak of τ_m/σ_m almost coincides with Mohr-Coulomb's criterion line. These indicators say that when the stress ratios, τ_h/σ_h and τ_m/σ_m , peak, the overall failure of a specimen occurs because Mohr's stress circle at this time contacts with Mohr-Coulomb's failure criterion line. Taking this together with the formation of local failure surfaces, as previously indicated, it is obvious that the failure of a specimen has a two-step failure mechanism, as the overall failure follows the formation of local failure surfaces. It appears that the overall failure doesn't occur at the time of the formation of local failure surfaces because the upper and lower loading plates of the specimen, which actually correspond to the upper soil mass and the lower ground of a shear band respectively, block a further development of these surfaces. Figure 11 shows Mohr's stress circle of the central element 3 at the time of overall failure of the specimen. It is seen in this figure that the horizontal plane almost agrees with the maximum shear stress plane. The agreement between these two planes is confirmed over a wide range of relative density, D_r , and K_0 -value (Tokue and Shigemura, 2003). Taking this together with the common use of Coulomb's failure criterion for a slip surface, which corresponds to the horizontal plane of a specimen or the boundary surface of a shear band, one of Coulomb's and Mohr-Coulomb's failure criteria can derive the other of the two under plane-strain condition as shown in Fig. 12.

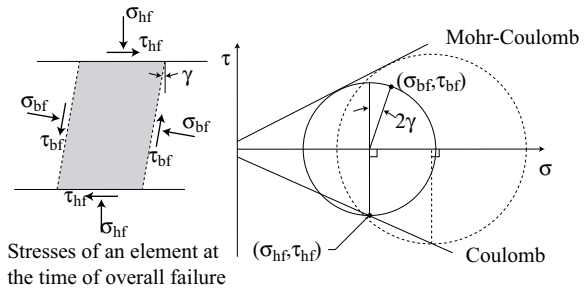


Figure 12. The relation between Coulomb's and Mohr-Coulomb's failure criteria

4 CONCLUSION

The simple shear tests using a large sand specimen with five-coupled elements, which excluded the influences of artificial boundaries of the specimen as much as possible and enabled interaction between soil elements, clarified the following main points about the failure mechanism and characteristics of the specimen:

- 1) The influences of the rotational moment due to shear and the artificial boundary of the specimen are found in both side elements, but are insignificant in the middle three elements because the interaction between soil elements seems to diminish these influences in the middle three elements. As a result, the middle three elements can show shear behaviours such as those expected in a shear band.
- 2) The middle three elements resist the applied shear load by forming a homogeneous stress state, especially the pure shear state from an early stage of shear by interaction between soil elements.
- 3) A number of local failure surfaces, which intersect perpendicular to the shearing direction, are formed in the specimen at an early stage of shear. The formation of these local failure surfaces, which is largely affected by K_0 -values, significantly influences the shear behaviours after this formation.
- 4) The specimen shows a two-step failure mechanism as the overall failure follows the formation of local failure surfaces.
- 5) The shear stresses acting on the upper and lower surfaces of a specimen become almost the maximum of all the shear stresses acting on every plane of the specimen at the time of an overall failure. As a result, one of Coulomb's and Mohr-Coulomb's failure criteria can derive the other of the two under plane-strain condition.

REFERENCES

- Cole, E. R. L. 1967. The behaviour of soils in the simple shear apparatus. *Ph. D. thesis, University of Cambridge*.
- Miura, K., Miura, S. and Toki, S. 1986. Deformation behaviour of anisotropic dense sand under principal stress axes rotation. *Soils and Foundations*, 26(1): 36-52.
- Nakata, Y., Hyodo, M., Murata, H. and Yasufuku, N. 1998. Flow deformation of sands subjected to principal stress rotation. *Soils and Foundations*, 38(2): 115-128.
- Oda, M. 1975. On the relation $\tau/\sigma_n = \kappa \tan \phi$ in the simple shear test. *Soils and Foundations*, 15(4): 35-41.
- Ochiai, H. 1975. The behaviour of sands in direct shear tests. *Soils and Foundations*, 15(4): 93-100 (in Japanese).
- Tokue, T. 1999. A new concept of solving ground failure problems and failure propagation phenomena. *Proceedings of 44-th geotechnical symposium*, the Japanese Geotechnical Society, Osaka, 161-166 (in Japanese).
- Tokue, T. and Shigemura, S. 2003. Progressive failure and failure criteria for soil in limit equilibrium analysis for slope stability. *Proceedings of the International Workshop on Prediction and Simulation Methods in Geomechanics (IWS-Athens 2003)*, ISSMGE, 85-88.